RESEARCH ARTICLE

Photodegradation of Oxytocin and Thermal Stability of Photoproducts

OLIVIER MOZZICONACCI, CHRISTIAN SCHÖNEICH

Department of Pharmaceutical Chemistry, University of Kansas, Lawrence, Kansas 66047

Received 15 February 2012; revised 27 April 2012; accepted 1 May 2012

Published online in Wiley Online Library (wileyonlinelibrary.com). DOI 10.1002/jps.23204

ABSTRACT: Photodegradation of oxytocin at $\lambda = 253.7$ nm and $\lambda \geq 290$ nm results in the transformation of the intrachain disulfide bond into predominantly dithiohemiacetal and thioether. Especially the dithiohemiacetal is sensitive to further degradation by light and/or elevated temperature, implying that the combination of an initial photostress and a subsequent heat stress can yield products significantly different compared with those observed under heat stress only. © 2012 Wiley Periodicals, Inc. and the American Pharmacists Association J Pharm Sci

Keywords: mass spectrometry; stability; oxidation; hormones; peptides

INTRODUCTION

Peptide hormones are active in various physiological processes and are critical for cell-signaling mechanisms. Oxytocin is a neuropeptide used as a therapeutic drug for stimulating labor, lactation, and to reduce the incidence of postpartum hemorrhage.[1–3] More recently, a role for oxytocin in therapeutic interventions in mental disorders associated with social deficits has been discussed.[4,5] The stability of oxytocin is pH dependent with an optimal pH between 3 and 5.[6,7] Degradation and specifically reduction–oxidation studies of oxytocin have been performed to demonstrate the cyclic structure of this neuropeptide.[8,9] Stability studies of oxytocin have shown that any injectable or solid formulation is rapidly degraded during storage under conditions of elevated temperature (>30°C) and humidity.[10,11] Several strategies have been developed to stabilize oxytocin, for example, stabilization by divalent metal ions.[12] Although the effects of physical and chemical[12,13] stresses on oxytocin (e.g., pH and temperature) were extensively studied, a detailed photodegradation study [under ultraviolet (UV) light] of oxytocin has never been reported. In a report on the stability of injectable oxytocics in tropical climates,[14] the World Health Organization (WHO) did not report any modifications of oxytocin under daylight exposure. However, in the same report, it is mentioned that oxytocin was protected from sunshine. UV wavelengths shorter than 290 nm are absorbed by molecular oxygen, ozone, and water vapor in the upper atmosphere, and do not reach the surface of the earth in measurable amounts. Thus, the WHO has reported in their Environmental Health Criteria[15] that all biologically important effects of sunlight are due to wavelengths $\lambda > 290$ nm. The spectral irradiance of sunlight between 290 and 380 nm is approximately between 0.5 and 1 W/(m^2 nm).[15] For comparison, in our photochemical study, the irradiance for $\lambda > 290$ nm is 60-fold to 100-fold higher than natural sunshine.

Here, we provide a product analysis of oxytocin exposed to UV light at $\lambda = 253.7$ nm and at $\lambda \geq 290$ nm. Photolysis at these wavelengths resulted in the transformation of the intrachain disulfide bond into a dithiohemiacetal structure, as expected based on our earlier studies with several model disulfides,[16] cyclic peptides,[17] insulin,[18] and IgG1.[19] Such dithiohemiacetals are photolabile and heat labile.[17] In fact, prolonged UV exposure or incubation of the dithiohemiacetal to elevated temperatures led to the formation of secondary products such as thioethers. All products of oxytocin photodegradation have been analyzed by mass spectrometry (MS), including (MS–MS) MS^2 and MS–MS–MS (MS^3) analysis. We discuss in detail the fragmentation pathways of the cyclic fragment ions obtained during MS^2 and MS^3 analysis. The characterization of cyclic peptide structures through

Additional Supporting Information may be found in the online version of this article. Supporting Information

Correspondence to: Christian Schöneich (Telephone: +785-864-4880; Fax: +785-864-5736; E-mail: schoneic@ku.edu)

Journal of Pharmaceutical Sciences

MS^n analysis presents two advantages: (i) to investigate the structure of products, which are not formed in sufficient amount for Nuclear Magnetic Resonance (NMR) analysis and (ii) to limit chemical steps to linearize the product prior to analysis.

MATERIALS AND METHODS

Materials

Ammonium bicarbonate (NH_4HCO_3), dithiothreitol (DTT), *N*-ethylmaleimide (NEM), and sodium dihydrogen and monohydrogen phosphate were supplied by Sigma–Aldrich (St. Louis, Missouri) at the highest purity grade. Oxytocin was purchased from Bachem (Torrance, California). The structure of oxytocin is presented in Chart 1.

Ammonium bicarbonate buffer was prepared at a concentration of 50 mM at pH 7.8. Sodium phosphate buffer was prepared at a concentration of 20 mM at pH 7.0. The reaction mixtures were either gently purged with Ar or left under air. UV irradiations at $\lambda = 253.7$ nm and $\lambda \geq 290$ nm were carried out by means of a photoirradiator (Rayonet™, Southern New England, Branford, Connecticut; RMA-500) equipped with four lamps (for $\lambda = 253.7$ nm, RPR-2500Å lamps were used; for $\lambda \geq 290$ nm, RPR-3000Å lamps were used). The RPR-3000Å lamps are characterized by a spectral distribution between 250 and 350 nm, with $\lambda_{max} = 300$ nm. However, the use of Pyrex® glass for irradiations at $\lambda_{max} = 300$ nm effectively filters out light with $\lambda < 290$ nm.[20] The total flux at $\lambda = 253.7$ nm was 3.2×10^{-7} einstein/s.

Methods

Photodegradation of Oxytocin

In a first experiment, oxytocin was dissolved to 20 mM phosphate buffer, pH 7.0, at a concentration of 250 μM. The solutions were either placed in quartz or Pyrex® tubes prior photoirradiation at $\lambda = 253.7$ nm or $\lambda \geq 290$ nm under Ar, respectively. In a second protocol, oxytocin powder provided by Bachem (in its acetate salt) was simply diluted in milliQ H_2O to reach a concentration of 700 μM. The pH was adjusted with HCl to be 4.0. The samples were photoirradiated at $\lambda = 253.7$ nm or $\lambda \geq 290$ nm in air, respectively.

Thermal Stability of Oxytocin

Oxytocin and oxytocin, which was photoirradiated at $\lambda \geq 290$ nm, were incubated overnight at 45°C.

Reduction of Disulfide Bonds and Alkykation of Products

After photoirradiation and/or incubation at 45°C, 200 μL of each sample were diluted with 800 μL of 50 mM NH_4HCO_3 buffer, pH 7.8. Fifty microliters of DTT (10 mM) were added to each sample for reduction of the disulfide bonds. The samples were incubated at 45°C for 30 min. Then, 150 μL of NEM (10 mM) were added to each sample to derivatize the thiol groups (including residual DTT). The samples were incubated at 45°C for 30 min.

Sample Preparation for Capillary Liquid Chromatography–MS Analysis

The samples were diluted (1/10) in milliQ H_2O. Sample (10 μL) was injected onto a Vydac column (25 cm × 0.5 mm C18, 3.5 μm), and eluted with a linear gradient delivered at the rate of 20 μL/min by a capillary liquid chromatography (LC) system (Waters Corporation, Milford, Massachusetts). Mobile phases consisted of water/acetonitrile (ACN)/formic acid at a ratio of 99%, 1%, 0.08% (v/v/v) for solvent A and a ratio of 1%, 99%, 0.06% (v/v/v) for solvent B. The following linear gradient was set: 1%–40% of solvent B within 20 min. Electrospray ionization–MS spectra of the photoproducts were acquired either on a SYNAPT-G2 (Waters Corporation) or an LTQ-FT hybrid linear quadrupole ion trap Fourier transform ion cyclotron resonance (FT-ICR) mass spectrometer (ThermoFinnigan, Bremen, Germany).[21] The SYNAPT-G2 was operated for maximum resolution with all lenses optimized on the $[M + 2H]^{2+}$ ion from the $[Glu]^1$-fibrinopeptide B. The cone voltage was 40 V and Ar was admitted to the collision cell. The spectra were acquired using a mass range of 50–2000 amu. The data were accumulated for 0.7 s per cycle. Collision-induced dissociation (CID) of fragment ions, referred to as MS^2 and MS^3, was performed on the FT-ICR (ThermoFinnigan).[21] MS^3 were acquired with an attenuation of the parent ion in the range of 45%–55%. The mass window to collect the parent ion was fixed to 0.2 Da.

Sample Preparation for High-Performance Liquid Chromatography Analysis–UV Detection

Non irradiated and UV-irradiated samples were analyzed in accordance with the European Pharmacopeia's protocol.[22] The samples were analyzed by means of a Shimadzu chromatographer (Shimadzu, Torrance, California) equipped with two pumps (LC-20AT; Shimadzu Prominance) delivering a flow rate of 0.9 mL/min, and a diode array detector (SPD-M20A; Shimadzu Prominance). The chromatographer was equipped with a Spherisorb column (4.6 × 250 mm, S5 ODS2; Waters Corporation). The analytes (50 μL injection volume) were eluted from the column with two eluents consisting of (i) sodium dihydrogen phosphate (0.1 M, solvent A) and (ii) H_2O/ACN (75%:25% (v/v), solvent B). The column was equilibrated with 70%:30% (v/v) of solvents A /B. The solvents were eluted with a linear gradient over a period of time of 30 min to reach a solvent composition of A:B 40%:60% (v/v).

 DOI 10.1002/jps

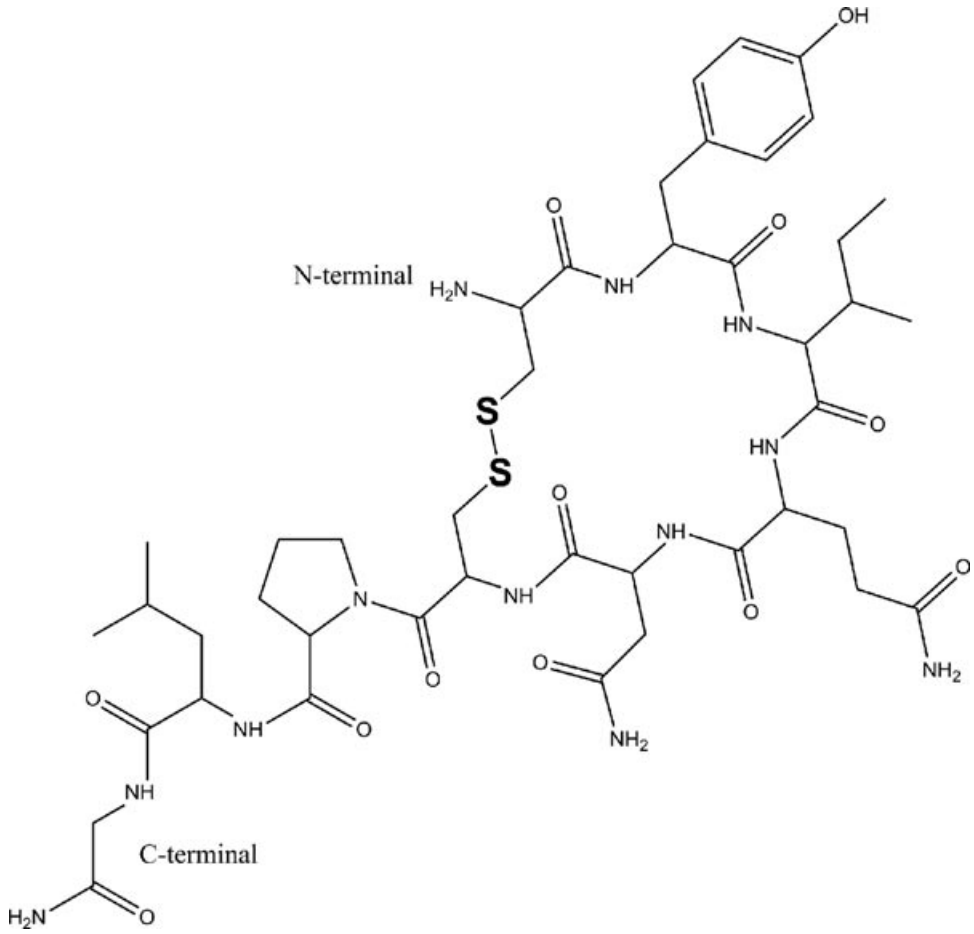

Chart 1. Structure of oxytocin.

RESULTS

For simplification, the structures of oxytocin (see below) and its photoproducts are represented in one letter code, where "S" refers to the sulfur atom (since the peptide sequence does not contain Ser). The tentative structures of the photoproducts, assigned based on MS/MS analysis, are presented in Table 1.

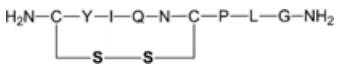

UV Irradiation of Oxytocin

Oxytocin (*m/z* 1007.4) was photoirradiated at λ = 253.7 nm and $\lambda \geq 290$ nm for 30 min in Ar- or air-saturated solution. The samples irradiated under Ar were analyzed by LC–MS (Fig. 1). Four major photoproducts, referred to as **1**, **2**, **3**, and **4**, were identified. The photoproducts were characterized by LC–MS/MS analysis and are tentatively assigned to the structures displayed in Table 1. The samples photoirradiated in air were analyzed by high-performance liquid chromatography (HPLC) coupled to UV detection ($\lambda = 230$ nm) according to the protocol reported in the European Pharmacopeia.[22] The major peaks were collected and analyzed by MS.

UV Irradiation Under Ar at $\lambda = 253.7$ nm

After UV irradiation of oxytocin (700 μM) under Ar at λ = 253.7 nm, products **1**, **2**, **3**, **4a**, and **4b** were observed. Analogous products have been detected after photoirradiation of a small cyclic disulfide-containing model peptide, for which a thioether, analogous to product **3**, and a dithiohemiacetal, analogous to product **2**, were supported by two-dimensioanal NMR analysis.[17]

Product 1. Product **1** is the result of the disproportionation of a pair of thiyl radicals into thiol and thioaldehyde, where the thioaldehyde has hydrolyzed into aldehyde (see *Discussion*, Scheme 1). The MS^2 spectrum of **1** allows to identify the aldehyde and the thiol group on the original N-terminal and C-terminal cysteines, respectively (Fig. 2). The b4, b6, y3, and y4 fragment ions demonstrate that the C-terminal cysteine is derivatized with NEM. The b4 fragment ion demonstrates the loss of 18 Da from the original N-terminal cysteine, consistent with the

Table 1. Overview of the Different Products Tentatively Assigned by Mass Spectrometry

Reference	Structure	Reference	Structure
1	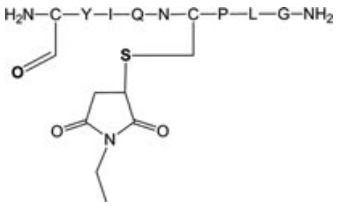	**4b**	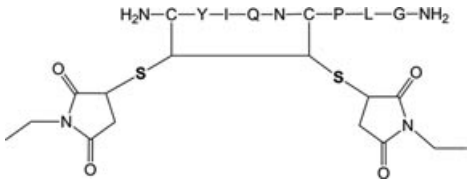
2	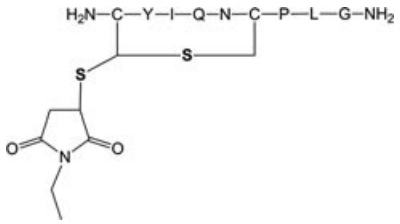	**5**	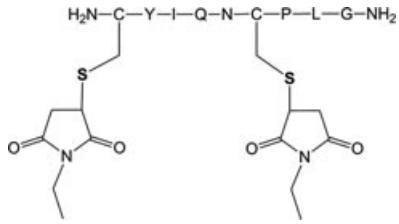
3	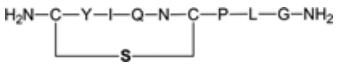	**6**	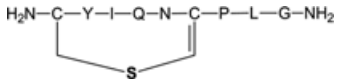
4a	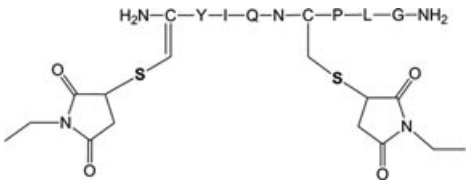		

The free thiol groups were derivatized with NEM. In products **4a** and **6**, the carbon–carbon double bond is located between the carbons C and $^{\beta}$C of Cys residue.

conversion of the Cys mercaptomethyl side chain into the aldehyde.

Product 2. Product **2** corresponds to the transformation of the disulfide bond into a dithiohemiacetal. Because of the presence of a non reducible C—S bond, the MS^2 spectrum of **2**, displayed in Figure 3, shows mainly the b6–b9 fragment ions. The loss of 159 Da from the b6 ion (*m/z* 689.2) is consistent with the loss of 1-ethyl-3-mercapto-pyrrolidine-2,5-dione, shown in the insert of Figure 3a. A proposed mechanism leading to the loss of 159 Da is detailed in Scheme S1 (Supplementary Information), along with the rationalization of the formation of the fragment ion with *m/z* 843.2, displayed in the zoom below the main spectrum in Figure 3b. From the parent ion (*m/z* 1132.5), the proton is transferred to the sulfur atom connected to NEM (Scheme S1, reaction S1-1). Such transfer allows the loss of 159 Da (reaction S1-2). The following addition of an amide to the carbocation permits the formation of a new mobile proton, which can transfer to the N-terminal amine (reactions S1-3 and S1-4), allowing the loss of NH_3 and the formation of the ion with *m/z* 956.5 (reaction S1-5). A subsequent rearrangement of the tetracyclic intermediate (reactions S1-6 and S1-7) allows to rationalize the next two steps. First, the formation of the acylium ion allows the loss of 28 Da and the formation of the ion with *m/z* 928.5 (reaction S1-7). Second, the formation of the carbon–carbon double bond permits a nucleophilic addition from any amide nitrogen (reaction S1-7). The latter creates a protonated amide bond, which can be cleaved (reaction S1-8) to permit the loss of CO (−28 Da, reaction S1-9) and the formation of the ion with *m/z* 900.3. The use of the C-terminal amide group in reaction S1-7 permits the loss of 57 Da (C_2H_3NO) in reaction S1-10, and the formation of the ion with *m/z* 843.2. In the MS^2 spectrum of 2 (Fig. 3), we tentatively assign the ion with *m/z* 928.5 to the b7 fragment, which lost NH_3, that is, b7-NH_3. However, the absence of the native b7 ion suggests that the ion with *m/z* 928.5 is more likely related to the fragmentation of the ion with *m/z* 956.5 as described above. Noteworthy, the ion with *m/z* 928.5 is part of the combination of the ions with *m/z* 956.5, 928.5, 900.2, and 843.2, which are necessary to explain the fragmentation mechanism depicted in Scheme S1. This series of ions supports the proposed mechanism presented in Scheme S1. Moreover, the cyclic structure of the ion with *m/z* 956.5, as displayed in Scheme S1, is supported by the fragment ions obtained during its MS^3 fragmentation (Fig. S1). Indeed, MS^3 of the ion with *m/z* 956.5 shows

 DOI 10.1002/jps

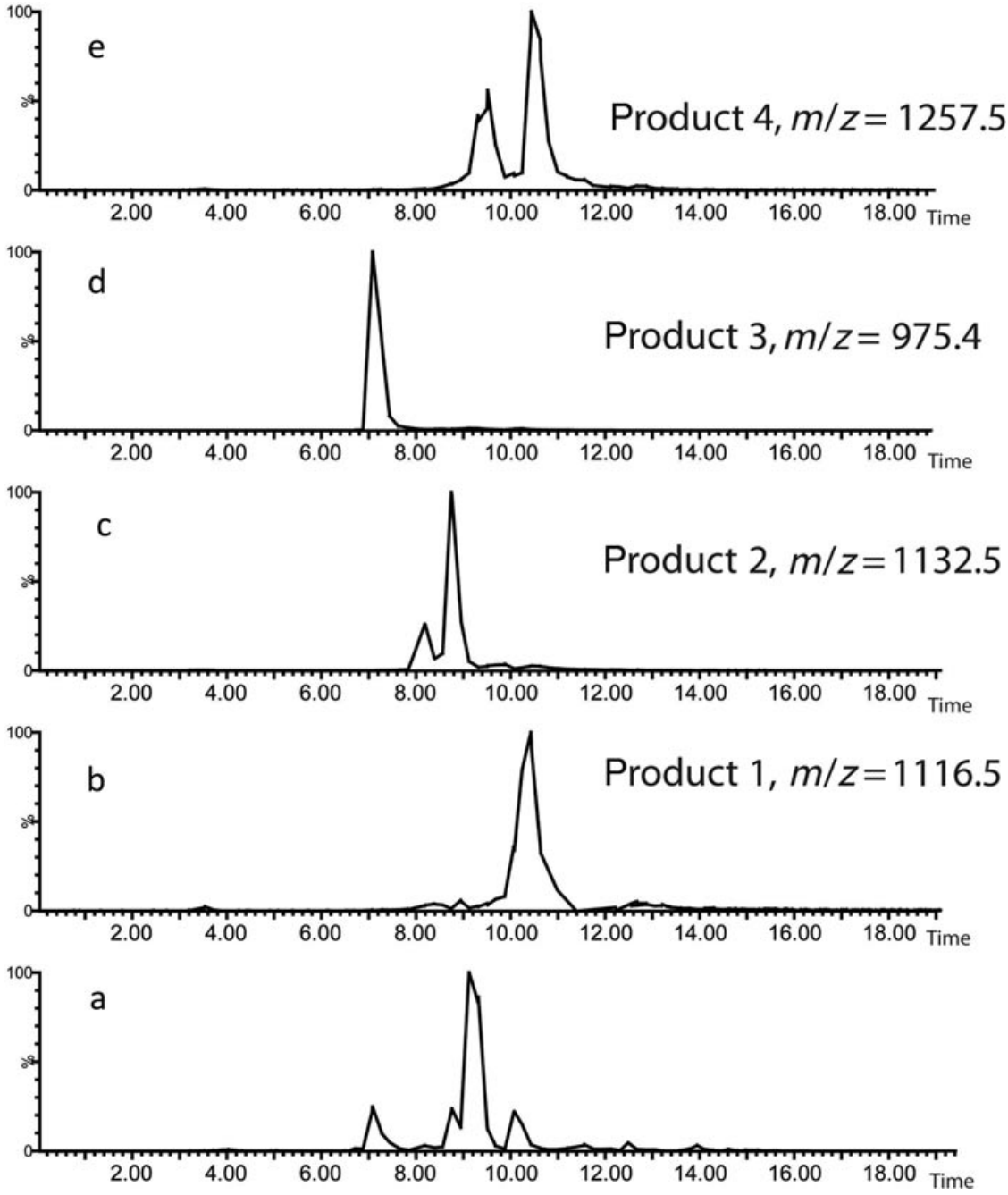

Figure 1. LC–MS analysis of photoirradiated oxytocin at $\lambda = 253.7$ nm under Ar. (a) Original LC–MS chromatogram displaying the different photoproducts. (b–e) Mass search ([M + H]) of the major products resulting from the photoirradiation of oxytocin. Disulfide bonds were reduced by DTT and derivatized with NEM.

a first series of ions with *m/z* 882.3, 769.4, and 672.1, corresponding to the loss of the residues Gly–NH_2 (Scheme S2, S2-2), Leu–Gly–NH_2 (Scheme S2, S2-3), and Pro–Leu–Gly–NH_2 (Scheme S2, S2-4) from the parent ion (*m/z* 956.5). These three fragments are easily removed from the parent ion since they are not part of the cyclic structure. Besides, after the loss of H_2S from the parent ion, the ion with *m/z* 922.4 is at the origin of the formation of the ions with *m/z* 714.2 and 601.3. Indeed, the difference of mass between 922.2 and 714.2 Da is 208 Da, which matches the sum of 163 + 45 Da. Thus, 208 Da is the combination of the masses of the monoisotopic masses of Tyr (163 Da) and an amide group ($CONH_3$, 45 Da). The loss of Tyr should be followed by the loss of Ile since the latter is adjacent to Tyr in the sequence of the parent ion (Scheme 1). The MS^3 analysis (Supplementary Fig. S1) indicates a difference of mass of 113 Da

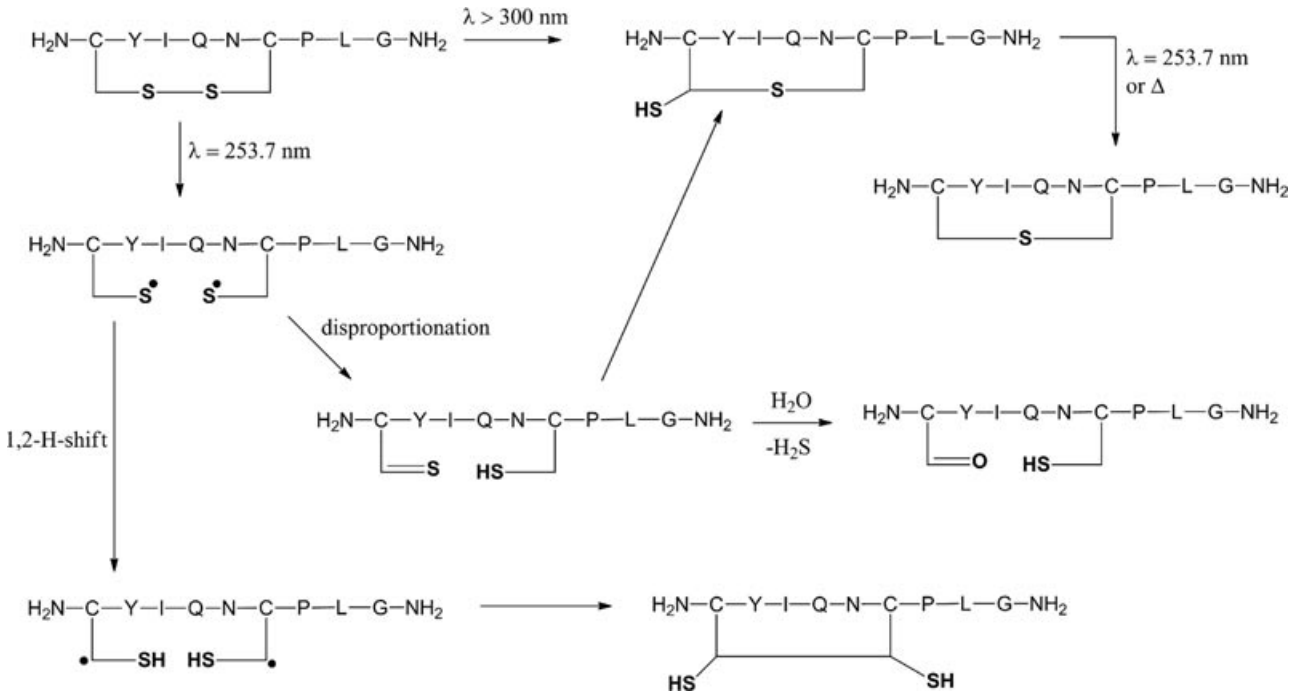

Scheme 1. Simplified reaction scheme summarizing the formation of the major photoproducts of oxytocin.

between the ions with *m/z* 714.2 and 601.3. This loss corresponds to the loss of Ile. The ions with *m/z* 714.2 and 601.3 are the result of a fragmentation occurring after the loss of H_2S from the parent ion. Thus, an opening of the thioether bond must precede the loss of Tyr and Ile. The mechanism to open the thioether bond during the MS^3 of the parent ion with *m/z* 956.5 is likely to be similar to the one that we will describe below to explain the MS^2 fragmentation of product **3** (Scheme S3, reaction S3-9 to S3-11).

Product 3. Product **3** corresponds to the transformation of the dithiohemiacetal (product **2**) into a thioether.[17] The structure of **3** is characterized by its MS^2 spectrum (Fig. 4). The presence of the b6–b9 and y3 fragment ions, as well the internal fragment YIQ and the absence of the other b fragments provide evidence for the formation of a thioether bond between the two cysteine residues. The ion with *m/z* 830.5 is rationalized through the mechanism displayed in Supplementary Scheme S3 (Supplementary Information). From the parent ion (*m/z* 975.4), the mobile proton can be transferred to the amide nitrogen that belongs to the peptide bond between the residues Ile and Gln (reaction S3-1). The amide group of the side chain of Gln can cyclize with the C-terminal side of Ile (reaction S3-2). At the same time, the primary amine which resulted from the cleavage of the peptide bond between Ile and Gln cyclizes with the carbonyl group of the side chain of Gln (reaction S3-3). So far, the mass of the ion has not changed, but the original cyclic peptide has opened. The formation of the ion with *m/z* 830.5 is the result of the loss of H_2S (34 Da). Thus, we need first to explain the intermediate ion with *m/z* 864.4. The latter must result from a loss of 111 Da from the parent ion. Thus, the ion formed after the reaction S3-3, which is isobaric to the parent ion, needs to be rearranged to allow further loss of the fragment with a mass of 111 Da, as described in reaction S3-8. Reactions S3-4 to S3-7 rationalize such rearrangement. An analogous rearrangement has been documented by Wysocki et al.[23] The intermediate ion formed through reaction S3-7 permits the neutral loss of 111 Da and the formation of the ion with *m/z* 864.4 (reaction S3-8). The protonated primary amine in the product ion allows for proton transfer to the sulfur atom (reaction S3-9). Subsequently, the original N-terminal opens the thioether bond and regenerates a free mobile proton (reaction S3-10). The transfer of the proton from the amine to the thiol group allows the protonation of the thiol function and the loss of H_2S (reactions S3-11 and S3-12) to generate the ion with *m/z* 830.5. To support the structure of the ion with *m/z* 830.5 as displayed in Supplementary Scheme S3, this ion was further fragmented in MS^3 experiments. The MS^3 spectrum of the ion with *m/z* 830.5 is presented in Supplementary Figure S2. Five fragment ions with *m/z* 813.1, 785.4, 717.2, 700.2, and 537.3 are generated. The formation of these ions is rationalized in Supplementary Scheme S4 (Supplementary Information). The formation of the series of ions with *m/z* 813.1, 785.4, and 700.2 corresponds to

 DOI 10.1002/jps

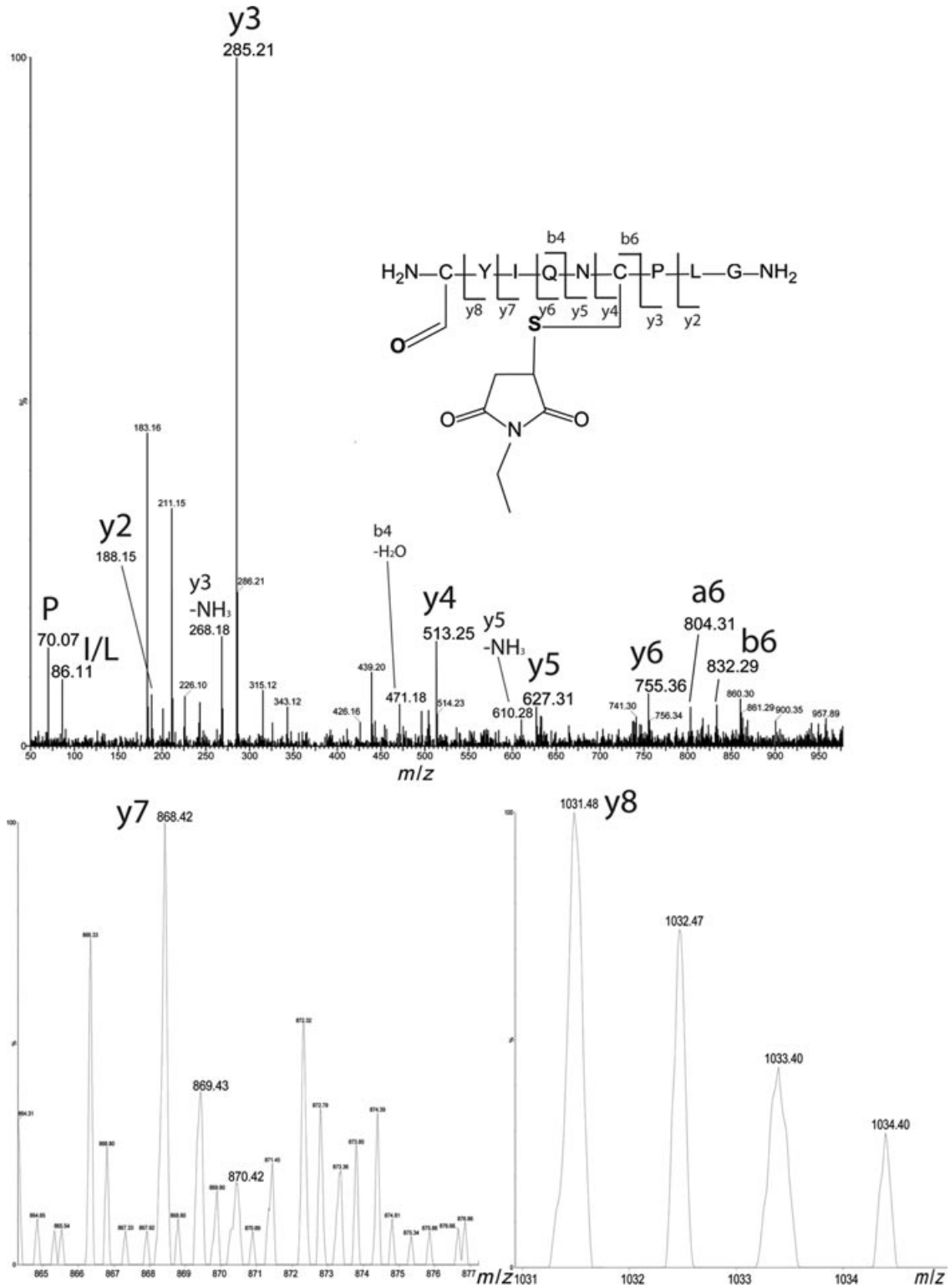

Figure 2. CID fragmentation of product **1** obtained on a SYNAPT-G2 mass spectrometer. Mass spectra at the bottom represent zoom-ins into the main mass spectrum (top).

the following fragmentation steps: (i) the loss of NH_3 from the parent ion (Scheme S4, reactions S4-1 to S4-3), (ii) the loss of CO (reaction S4-4), and (iii) the loss of the 2-methylbutan-1-imine (reaction S4-5). The difference of mass between the ions with *m/z* 830.5 and 717.2 is 113 Da and corresponds to the monoisotopic mass of Leu or Ile. The loss of Ile must be preceded by the loss of NH_3, as it is explained through reactions S4-1 to S4-3. Therefore, the direct loss of 113 Da from the parent ion cannot match the loss of Ile.

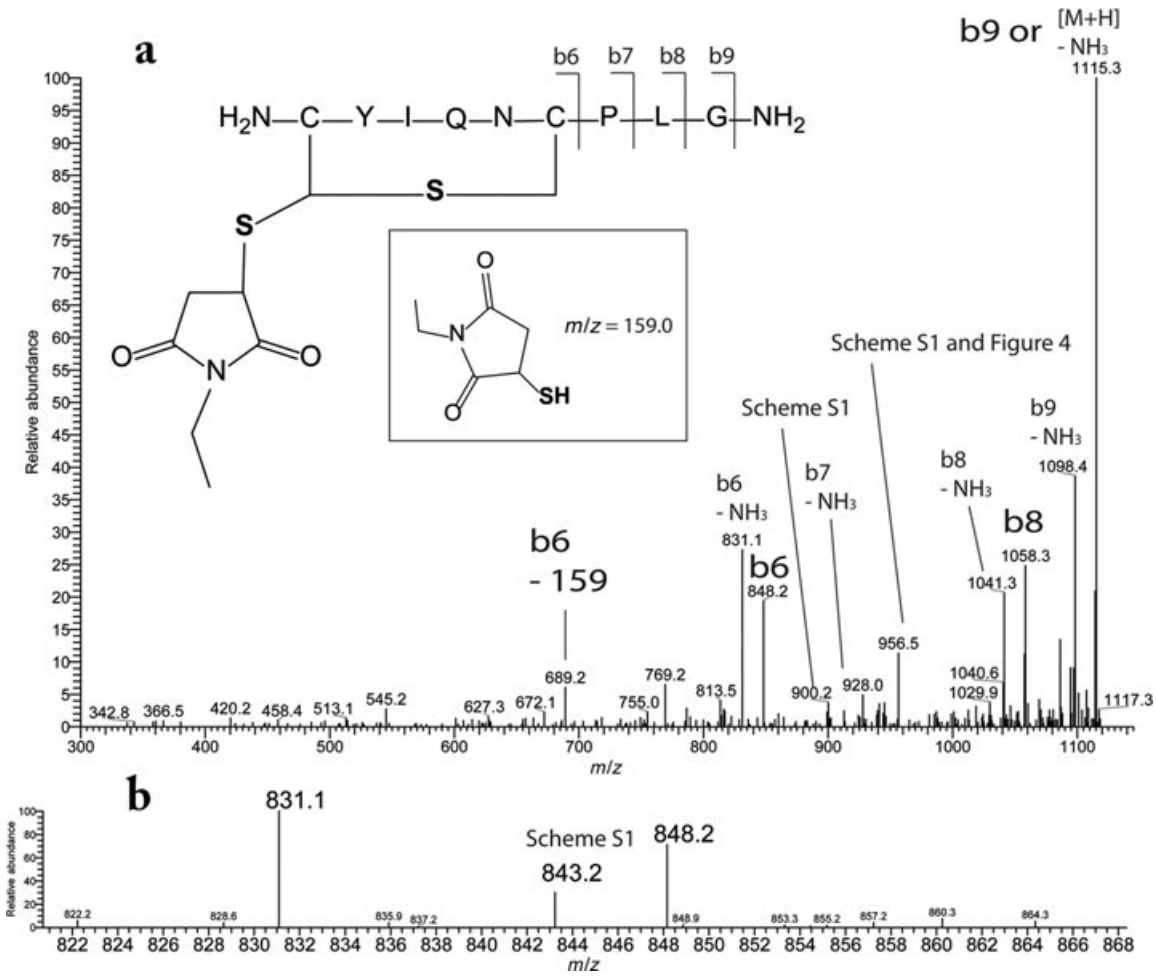

Figure 3. CID fragmentation of product **2** obtained on an FT-ICR mass spectrometer. Mass spectrum at the bottom represents zoom-in into the main mass spectrum (top).

Consequently, the loss of 113 Da from the parent ion can only be rationalized through the loss of the monoisotopic mass of Leu. The cyclization of the amide group of Gly with the carbocation present in the original parent ion (reaction S4-6) generates a free mobile proton permitting the protonation of the amide bond of Gly (reaction S4-7) and the internal fragmentation (reactions S4-8 and S4-9), which allows the release of Leu. The last fragment ion with *m/z* 537.3 (Supplementary Fig. S2) corresponds to the loss of Tyr–Ile–NH_2. This fragmentation is the result of the protonation of the amide bond of Tyr (reactions S4-10 and S4-11).

Products 4a and 4b. Products **4a** (Fig. 5a) and **4b** (Fig. 5b) are isobaric. In comparison to product **5** (*m/z* 1259.5) for which a description will be given below, **4a** and **4b** correspond to a loss of 2 Da from oxytocin. The loss of 2 Da can either be explained through the formation of a vinylic carbon–carbon bond such as in **4a** or the formation of a covalent carbon–carbon bond between the $^{\beta}$C carbons of the cysteines residues such as in product **4b** (theoretically, such coupling can also involve the $^{\alpha}$C carbons of Cys, but steric reasons likely prevent such a coupling).

In the MS^2 spectrum presented in Figure 5b, the fragment ions with *m/z* 513.1, 627.3, 755.2, and 868.3 can be assigned to the y4, y5, y6, and y7 fragment ions of product **4a**. However, their intensities are not comparable to the intensities of the same ions observed during the fragmentation of **5** (see below), suggesting that structure of **4b** rather than **4a** is formed. An analogous product was observed after photoirradiation of a cyclic disulfide-containing model peptide.[17]

UV Irradiation Under Air

Oxytocin (700 μM) was prepared by diluting the Bachem powder in milliQ H_2O. The pH of the solution was adjusted to 4.0 by using HCl solution. The samples were prepared by placing 200 μL of the stock solution in either quartz or Pyrex® tubes (opened to air) prior to UV irradiation at $\lambda = 253.7$ nm or $\lambda \geq 290$ nm, respectively.

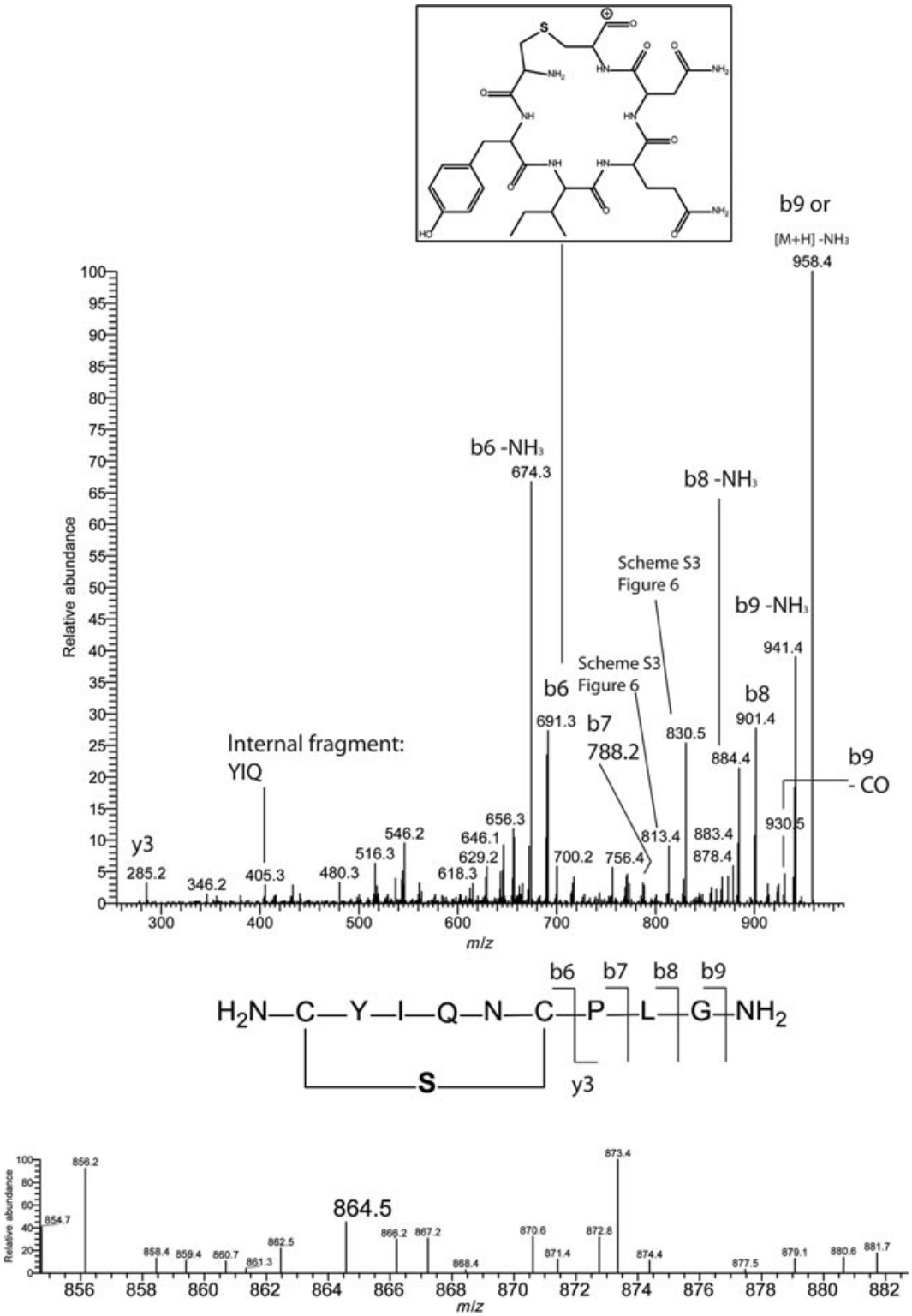

Figure 4. CID fragmentation of product **3** obtained on a FT-ICR mass spectrometer. Mass spectrum at the bottom represents zoom-in into the main mass spectrum (top).

Irradiation at λ = 253.7 nm. Oxytocin was exposed to UV light (λ = 253.7 nm) for 0, 5, 15, 30, and 60 min. The chromatograms of the non irradiated and irradiated samples are presented in Figure 6a. Native oxytocin is eluted after t_r = 14.9 min. Over the time of irradiation, oxytocin was transformed into product **3** (thioether), which is eluted at t_r = 9.7 min (Fig. 6a, peak 2). Peak 2 was collected for MS

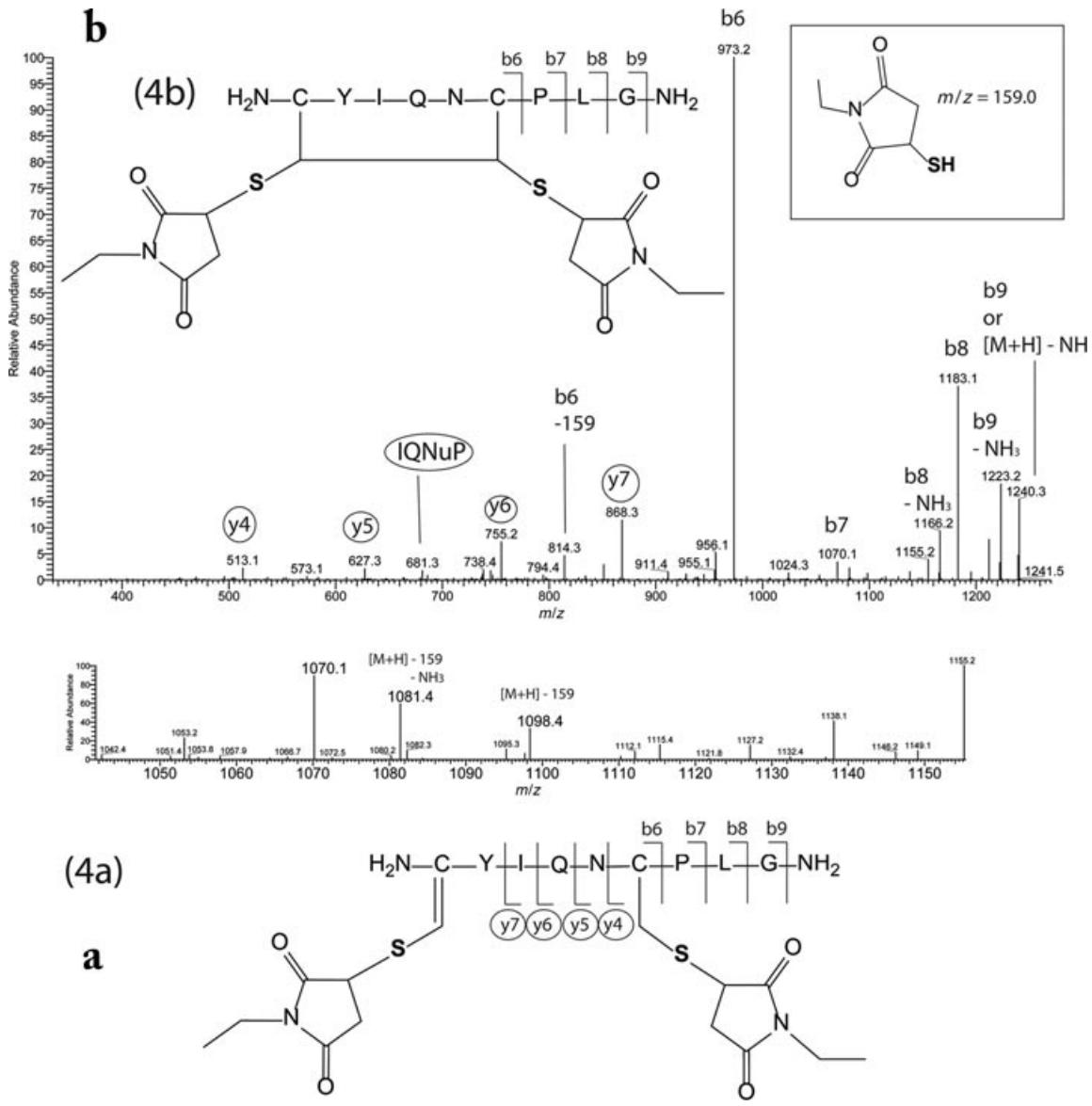

Figure 5. CID fragmentation of **4a** and **4b** obtained on a FT-ICR mass spectrometer. Mass spectrum at the bottom represents zoom-in of the main mass spectrum (top). "u" refers to the derivatization of Cys with NEM. The fragment ions in circles are related to the fragmentation of product **4b**. All the other ions are common to both products **4a** and **4b**.

analysis that revealed a mass-to-charge ratio of 975.5, isobaric to product **3** (Supplementary Fig. S4a).The relative abundance of oxytocin and product **3** was monitored over 30 min of irradiation (Fig. 6b). Within 30 min of UV exposure, the amount of oxytocin decreased linearly as the amount of product **3** increased. Over 30 min of UV exposure, oxytocin was completely transformed into **3**. However, a prolonged irradiation of product **3** in air induced its degradation into unknown photoproducts, which were eluted between 2 and 8 min.

Irradiation at $\lambda \geq 290$ *nm.* Oxytocin was exposed to UV light ($\lambda \geq 290$ nm) for 0, 5, 15, 30, and 60 min. The chromatograms of the non irradiated and irradiated samples are presented in Figure 6c. Native oxytocin is eluted after $t_r = 14.9$ min. Over 60 min of UV exposure, we did not observe the formation of an additional peak except the one assigned to the native oxytocin. However, over the time of UV irradiation, the absorption intensity (monitored at $\lambda = 230$ nm) of peak 1 decreased (Fig. 6c). MS analysis revealed that the mass-to-charge ratio of the product(s) eluted at $t_r = 14.9$ min was isobaric to the native oxytocin (*m/z* 1007.4, Supplementary Fig. S4b). We therefore assumed that the decrease of the absorption intensity of peak 1 over the time of irradiation could be related to the transformation of oxytocin into its dithiohemiacetal derivative (product **2**, where the free thiol is not

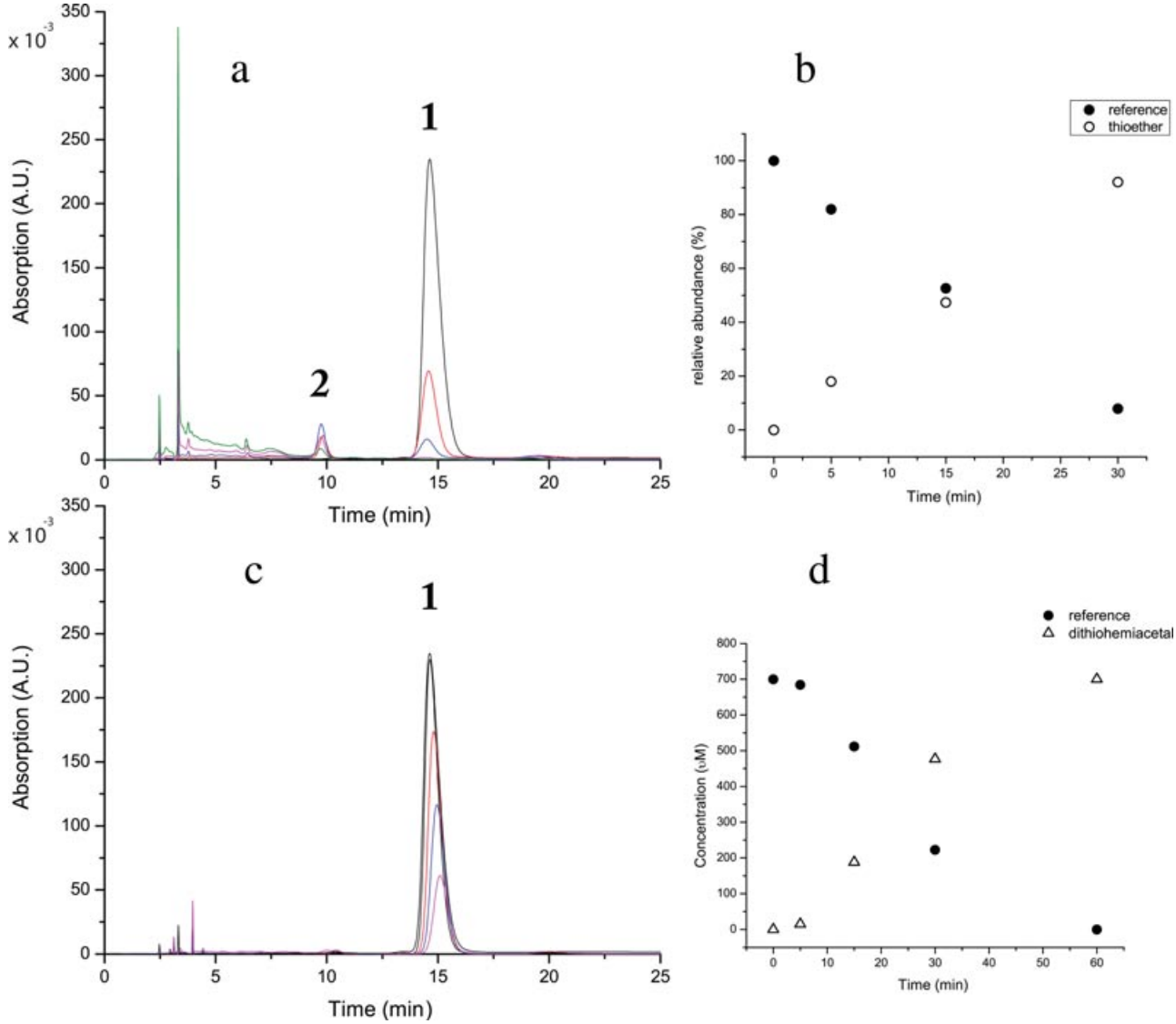

Figure 6. HPLC/UV-detection ($\lambda = 230$ nm) analysis of oxytocin. a)Oxytocin was UV-irradiated at $\lambda = 253.7$ nm in air for 0 min (black), 5 min (red), 15min (blue), 30 min (pink), 60 min (green). b) Monitoring of the conversion of oxytocin (●) (peak 1, a) into its thioether derivative (○) (product **3**, peak 2, a). c) Oxytocin was UV-irradiated at $\lambda > 290$ nm in air for 0 min (black), 5 min (red), 15 min (blue), 30 min (pink), 60 min (green). d) Monitoring of the transformation of oxytocin (●) into its dithiohemiacetal derivative (△) (product **2** (non derivatized with NEM), peak 1, c).

derivatized with NEM). To confirm such hypothesis, the oxytocin sample irradiated for 60 min was derivatized with NEM (Fig. 7). The chromatograms presented in Figure 7 show that the non irradiated oxytocin is not derivatized with NEM (Figs. 7a and 7b), where, after 60 min of UV exposure and NEM derivatization, a new peak appeared ($t_r = 17.8$ min, Fig. 7c) with an absorption approximately 10-fold higher than the absorption of peak 1 presented in Figure 6c. The higher intensity of the absorption is likely due to the conjugation of the maleimide group to the oxytocin photoproduct. To confirm the addition of NEM to the photoproduct, the new product eluted at $t_r = 17.8$ min (peak 2, Fig. 7c) was collected for MS analysis. The latter revealed that the product is isobaric to product **2** (*m/z* 1132.5, Supplementary Fig. S4c). Because the non-irradiated oxytocin was not derivatized by NEM, we assume that the NEM derivatization with the photoproduct is due to the presence of a free thiol, as in a dithiohemiacetal structure. Thus, in Figure 6c, the observation of the decrease of the absorption intensity of peak 1 over the time of irradiation is likely due to the transformation of the disulfide bond of oxytocin into a dithiohemiacetal structure (product **2**). The decrease of the absorption intensity can be rationalized by a smaller molar extinction coefficient at $\lambda = 230$ nm of

the dithiohemiacetal structure in comparison to the disulfide bond. The calculation of the absorption of the mixture of the dithiohemiacetal product and oxytocin can be linearized through Eq. 1 (for 0 min < t < 60 min, light pathway l = 1 cm; see equations below). At the particular time points, t = 0 min and t = 60 min, we assume that the measure of the absorption is only due to either the oxytocin or product **2** (where the free thiol is not derivatized with NEM), respectively (Eqs. 2 and 3). Through Eqs. 2 and 3, we can calculate the values of the molar extinction coefficients $\varepsilon_1{}^{230}$ and $\varepsilon_2{}^{230}$ ($\varepsilon_1{}^{230} = \varepsilon_{\text{disulfide}} + \varepsilon_{\text{aromatic}}$, $\varepsilon_2{}^{230} = \varepsilon_{\text{dithiohemiacetal}} + \varepsilon_{\text{aromatic}}$) at $\lambda = 230$ nm for oxytocin and product **2** (where the free thiol is not derivatized with NEM), respectively. Thus, $\varepsilon_1{}^{230}$(oxytocin) = 360 M/cm, and $\varepsilon_2{}^{230}$(product **2**) = 72 M/cm.[1] A combination of Eqs. 1 and 4 allows for the determination of the Eqs. 5 and 6, which control the concentration of product **2** (where the free thiol is not derivatized with NEM) and oxytocin over the time of irradiation, respectively (Fig. 6d).

$$A_t = \varepsilon_1^{230}[\text{oxytocin}]_t + \varepsilon_2^{230}[\text{product 2}]t \qquad (1)$$

where

$$\begin{aligned} \varepsilon_1^{230} &= \varepsilon_{\text{disulfide}}^{230} + \varepsilon_{\text{aromatic}}^{230} \text{ and } \varepsilon_2^{230} \\ &= \varepsilon_{\text{dithiohemiacetal}}^{230} + \varepsilon_{\text{aromatic}}^{230} \\ \text{at } t &= 0 \text{ min} : \\ A_0 &= \varepsilon_1^{230}[\text{oxytocin}]_0 \\ \text{at } t &= 60 \text{ min} \end{aligned} \qquad (2)$$

$$A_{60} = \varepsilon_2^{230}[\text{product 2}]_{60} = \varepsilon_2^{230}[\text{oxytocin}]_0 \qquad (3)$$

$$[\text{oxytocin}]_0 = [\text{oxytocin}]_t + [\text{product 2}]_t \qquad (4)$$

$$\text{For } 0 < t < 60 \text{ min}, :$$

$$[\text{product 2}]_t = 8.75\,10^{-4} - \frac{A_t}{288} \qquad (5)$$

$$\text{For } 0 < t < 60 \text{ min}, :$$

$$[\text{oxytocin}]_t = \frac{A_t}{288} - 1.75\,10^{-4} \qquad (6)$$

Thermal Stability of Photoirradiated Oxytocin

Oxytocin was photoirradiated at $\lambda \geq 290$ nm for 30 min in Ar and air. Control oxytocin and photoirradiated oxytocin were then incubated overnight at 45°C. LC–MS analyses of the samples pre-irradiated in Ar are presented in Figure 8. Three major products, referred to as **2**, **5**, and **6**, were identified (Table 1).

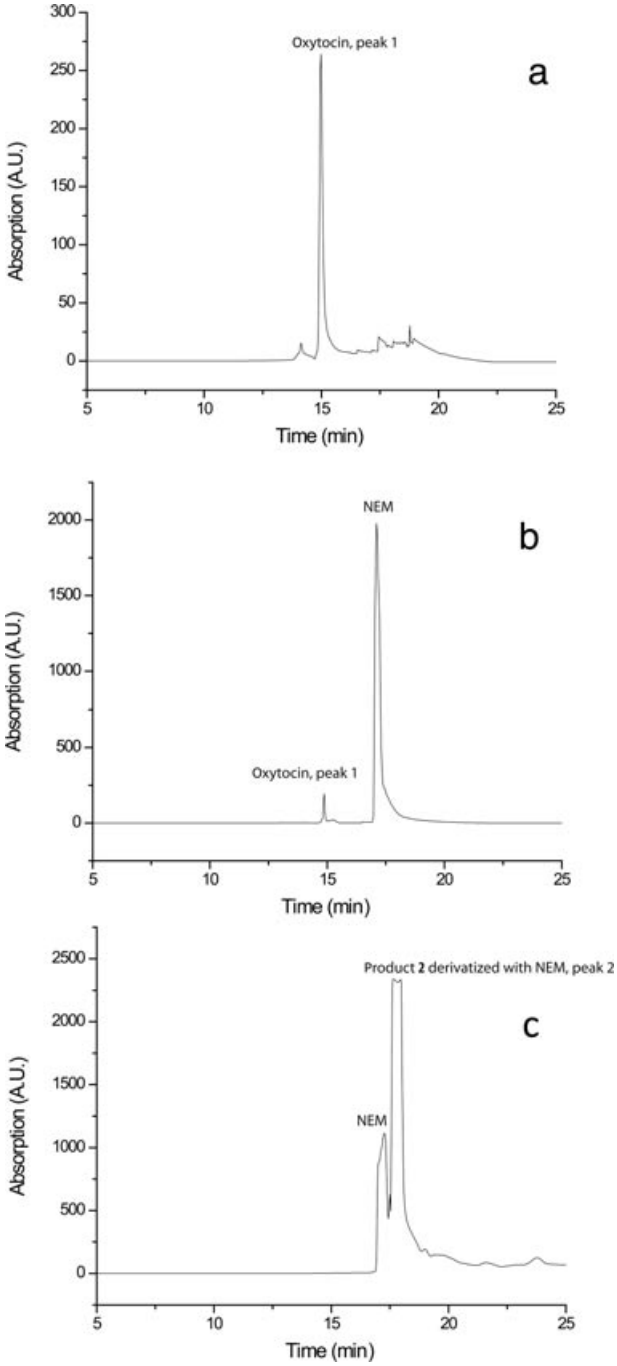

Figure 7. HPLC UV-detection ($\lambda = 230$ nm) analysis of oxytocin. a) Native oxytocin. b) Native oxytocin mixed with NEM. c) Oxytocin was UV-irradiated at $\lambda > 290$ nm in air for 60 min and derivatized with NEM.

Thermal Stability After Photoirradiation at λ > 290 nm Under Ar

The sample photoirradiated under Ar at $\lambda > 290$ nm was subjected to thermal stability testing. The sample was maintained in Ar during incubation. The LC–MS

[1] The molar extinction coefficients $\varepsilon_1{}^{230}$ and $\varepsilon_2{}^{230}$ are deduced from the absorption read at $\lambda = 230$ nm on the absorption spectra recorded during HPLC analysis. Therefore, at $t_r = 14.9$ min, the molecular extinction coefficients have been calculated in a solvent composition consisting of 45 mM NaH_2PO_4 in 72.5%:27.5% H_2O:ACN.

 DOI 10.1002/jps

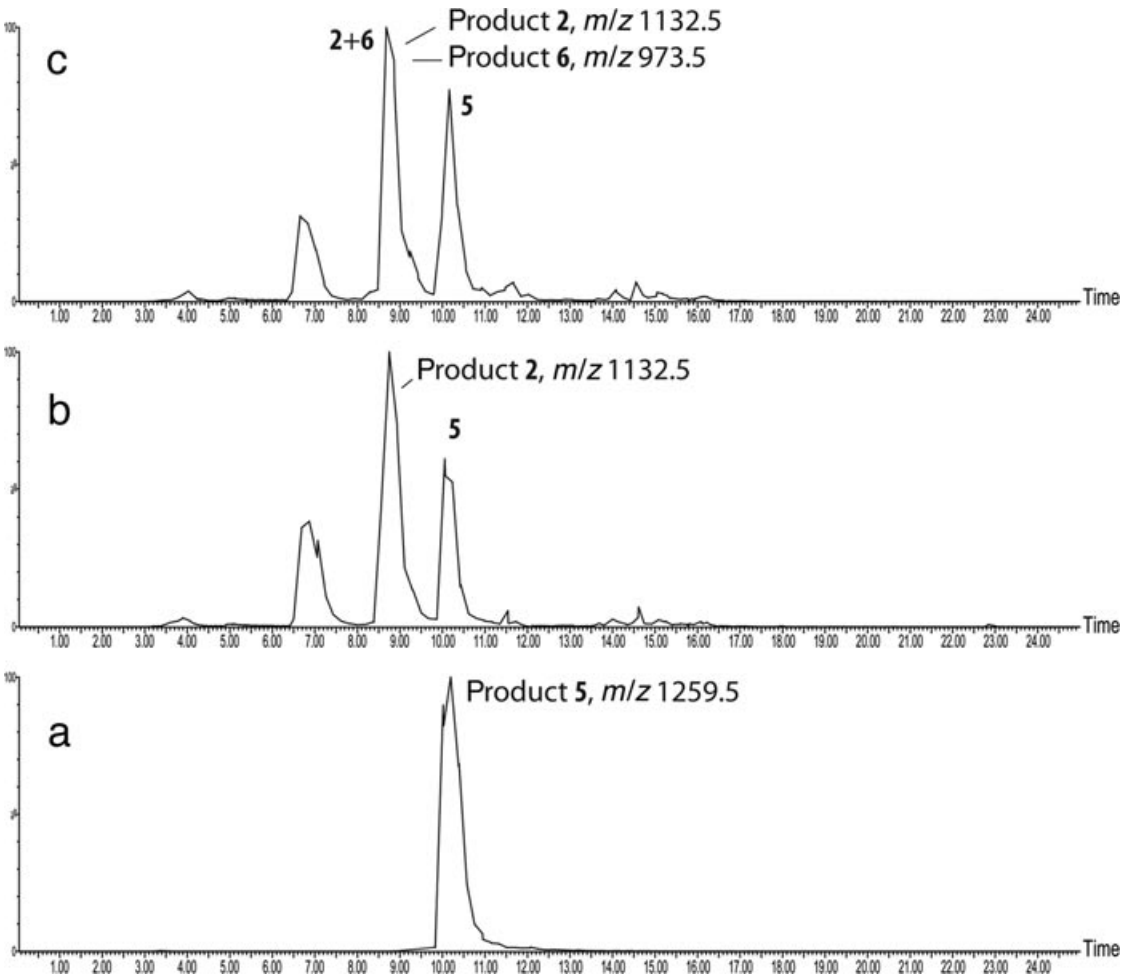

Figure 8. LC-MS analysis of oxytocin a)after DTT reduction and NEM derivatization, b) after photo-irradiation at $\lambda > 290$nm under Ar following by DTT reduction and NEM derivatization, c) after photo-irradiation at $\lambda > 290$ nm under Ar and overnight incubation at 45°C in Ar, followed by DTT reduction and NEM derivatization. Peak eluted at 7 min corresponds to molecules of DTT derivatized with two molecules of NEM.

analysis revealed the presence after incubation of two major products referred to as **5** and **6**.

Product 5. Product **5** is independently produced by reduction of oxytocin with DTT and alkylation of the free thiols by NEM. The MS^2 spectrum of **5** (Supplementary Fig. S3) provides evidence for its linear structure and the derivatization of the cysteine residues by NEM. The b2–b9, y4–y7, and the internal fragment ions QNu and IQNuP characterize the structure of **5** (here, u refers to the residue Cys–NEM). The ion with *m/z* 1225.3 needs further explanation. This ion is the result of a loss of 34 Da, most likely H_2S, from the parent ion (*m/z* 1259.5). Because the thiol functions are blocked by derivatization with two maleimide structures, the loss of H_2S needs to be rationalized (Supplementary Scheme S5). After protonation of the carbonyl oxygen of NEM, the N-terminal amine can cyclize with NEM into a hexacyclic structure (reaction S5-1 and S5-2). The mobile proton present on the amine can be transferred to the sulfur, leading to the formation of a free thiol group and a carbocation (reaction S5-4). Then, the proton of the alcohol function can be transferred to the secondary amine creating a new protonated amide bond (reaction S5-5). The mobile proton present on the nitrogen permits, after its transfer to the thiol group, the release of H_2S (reactions S5-6 and S5-7).

Product 6. Product **6** is observed after photoirradiation of oxytocin at $\lambda > 290$ nm, followed by incubation at 45°C. Product **6** shows similar MS^2 fragmentation (Fig. 9) as the thioether, product **3.** The presence of the b6 and y3 fragment ions provides evidence for the cyclization between the cysteine residues. However, the comparison of the mass-to-charge ratios of the y3, b6, and b7 fragment ions with those produced during the MS^2 fragmentation of the thioether, product **3**

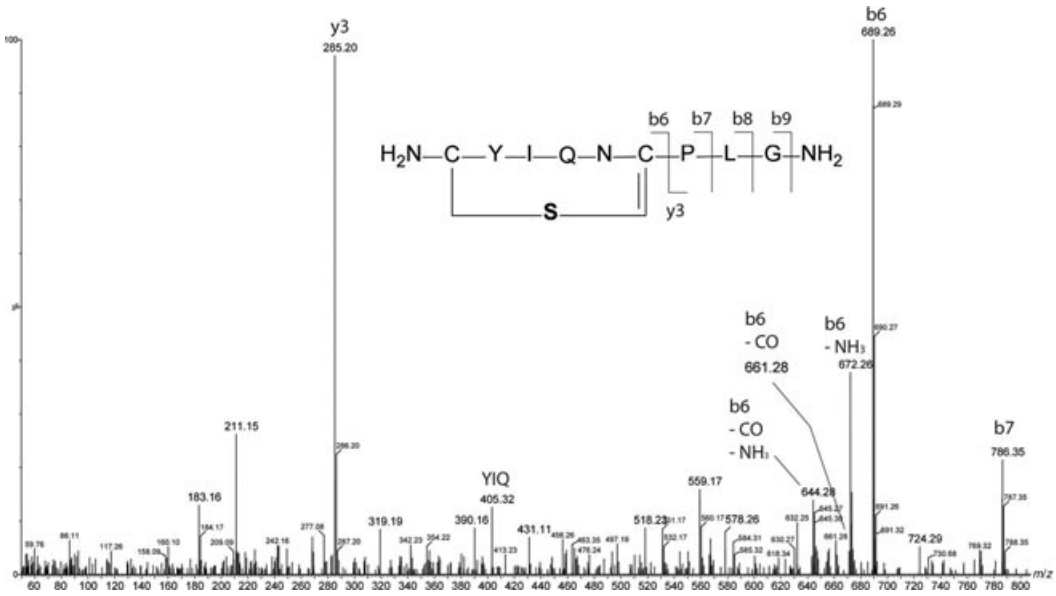

Figure 9. CID fragmentation of **6** obtainedon a SYNAPT-G2mass spectrometer.

(Fig. 4), show clearly a difference of −2 Da, supporting the formation of a vinylic group. An analogous vinyl–thioether structure was detected upon photoirradiation of other cyclic-containing model peptides.[17]

Thermal Stability After Photoirradiation at λ> 290 nm Under Air

The sample photoirradiated in air at $\lambda > 290$ nm for 30 min was subjected to thermal stability testing. UV detection revealed the complete transformation of the photoproducts and oxytocin into new species coeluted after 30 min (Fig. 10). The photo- and heat-stressed sample was subjected to MS analyses in different ways: (i) the sample was immediately analyzed by MS; (ii) after heat stress, the sample was mixed with DTT in NH_4HCO_3 buffer (pH 7.8, 50 mM) prior to analysis by MS. MS analysis of these samples revealed the presence of products with molecular weights higher than that of oxytocin (Supplementary Fig. S5). No significant difference was observed in the range of masses monitored by MS after mixing the stressed sample with DTT. Thus, the high–molecular-weight products are non reducible, meaning that no disulfide structure has survived the photo and thermal stresses. The high-molecular-weight species likely involve multiple combinations of modifications, where preliminary data would be consistent with tyrosine oxidation, cross-linking of tyrosine oxidation products with thiol or amine residues, and a possible hydrolytic cleavage at Pro. Future experiments will be designed to investigate the nature of these non reducible cross-links.

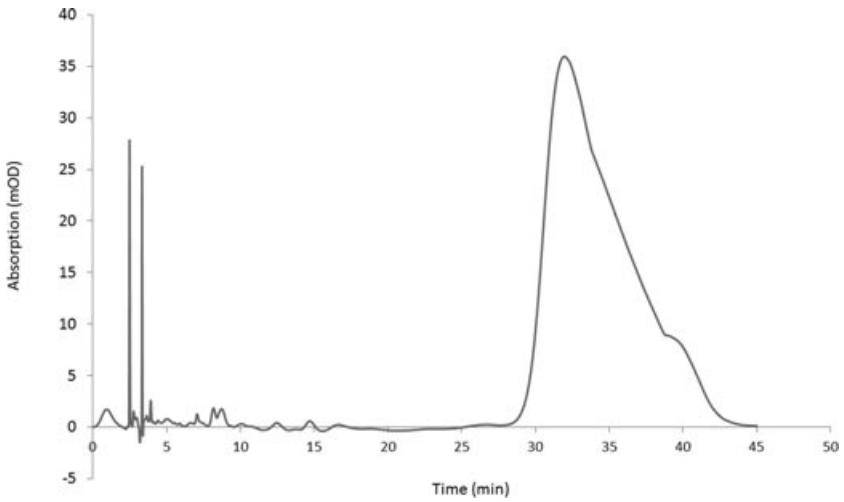

Figure 10. HPLC UV-detection ($\lambda = 230$ nm) analysis of oxytocin after UV-irradiation at $\lambda > 290$ nm in air and incubation at 45°C overnight.

DISCUSSION

To assist in the following discussion, a simple reaction scheme is presented in Scheme 1.

The photodegradation of oxytocin at $\lambda = 253.7$ nm and $\lambda \geq 290$ nm leads to the formation of stable photoproducts identified by MS. The absorption of light by a disulfide bond (λ_{max} ca. 250 nm) results initially in the formation of a pair of cysteinyl radicals (CysS$^{\bullet}$).[24] In the singlet state, the pair of CysS$^{\bullet}$ radicals can recombine to regenerate the disulfide bond. However, rapid intersystem crossing will efficiently generate a triplet radical pair of CysS$^{\bullet}$ radicals.[25] In the triplet state, the parallel spins of the CysS$^{\bullet}$ radicals prevent such recombination. Thus, in the triplet state, the two CysS$^{\bullet}$ radicals will most likely disproportionate to yield a thiol and a thioaldehyde.[26,27] In H_2O, the thioaldehyde is rapidly transformed into aldehyde, explaining the formation of **1**. We demonstrated with an intrachain disulfide-containing model peptide and with salmon calcitonin that such disproportionation reaction occurred.[17] However, in the particular case of an intrachain disulfide bond, the disproportionation products can rapidly convert into a dithiohemiacetal (product **2**).[17] In product **2**, the S—C—S structure is similar to that in 1,3,5-trithiane and 1,3-dithiane. Steady-state and laser flash photolysis studies of derivatives of 1,3,5-trithiane have shown the formation of radical or ionic species through homolytic or heterolytic cleavages of the C—S bond.[28–31] This observation suggests that the structure S—C—S in product **2** is photosensitive at $\lambda = 253.7$ nm, consistent with our earlier data on the photosensitivity of dithiohemiacetal of a cyclic model peptide.[17] Thus, the continuous exposure of **2** (where the free thiol is not derivatized with NEM) at $\lambda = 253.7$ nm leads to the formation of product **3**. In addition, we observed that the incubation of the dithiohemiacetal photoproduct of oxytocin leads to the formation of product **6**. Such observation is consistent with our previous study where we reported that a dithiohemiacetal structure is not only photosensitive but also heat labile.[17] Our results show that the HPLC methodology recommended in the pharmacopeia to study the stability of oxytocin cannot discriminate native oxytocin from its dithiohemiacetal derivative.

Our MS^2 data do not provide sufficient detail to distinguish the isobaric structures **4a** and **4b**. However, we know that the formation of a biradical molecule may lead to the formation of product **4b**. Indeed, a formal 1,2-H-shift reaction occurring in each of the CysS$^{\bullet}$ radicals would generate two $^{\beta}$C carbon-centered radicals, which ultimately would react together to form a C—C bond. The formation of product **4b** and the observation of a similar structure during photo-irradiation of an intrachain disulfide-containing model peptide support the occurrence of such 1,2-H-shift processes.[17]

On the basis of our previous experiments with an intrachain disulfide-containing model peptide and salmon calcitonin, we know that if the photoirradiation at $\lambda = 253.7$ nm is maintained under Ar flow, the disulfide bond is exclusively transformed into a thioether.[17] With oxytocin, we made a similar observation. The photoirradiation of oxytocin at $\lambda = 253.7$ nm under Ar flow generates exclusively product **3**. An important observation is the temperature–sensitivity of the photoproducts, especially of the dithiohemiacetal **2**. For practical purposes, that means that any exposure of oxytocin to elevated temperature may yield significantly different products when such peptide had been exposed to light prior to storage at elevated temperature.

The studies under Ar atmosphere allowed us to determine critical photoproducts generated during UV light stress of oxytocin. The structures of the photoproducts generated under air are similar to those observed under Ar. The major differences observed between experiments under Ar and air occur during subsequent heat stress. When the photoproducts are incubated in the presence of air, we observed the formation of non reducible high–molecular-weight products likely combining different types of modifications (e.g., oxidation of Tyr, cross-linking, and hydrolytic cleavage).

CONCLUSION

Our study shows that at pH 4.0–5.0 or pH 7.0–8.0, oxytocin is sensitive to UV light. Oxytocin is easily transformed in presence of Ar or air into its thioether and dithiohemiacetal derivatives after UV exposure at $\lambda = 253.7$ nm and $\lambda > 290$ nm, respectively. Under inert atmosphere, the combination of light and heat stresses leads to the transformation of the disulfide bond of oxytocin into a thioether. Under air, subsequent heat stress leads to the formation of non reducible cross-links.

ACKNOWLEDGMENTS

We gratefully acknowledge financial support from Amgen Inc.

REFERENCES

1. Dale HH. 1906. On some physiological actions of ergot. J Physiol 34(3):163–206.
2. Schafer EA, Mackenzie K. 1911. The action of animal extracts on milk secretion. Proc R Soc London, Ser B 84:16–22.
3. Ott I, Scott JC. 1910. The action of infundibulum upon mammary secretion. Proc Soc Exp Biol 8:48–49.
4. Andari E, Duhamel JR, Zalla T, Herbrecht E, Leboyer M, Sirigu A. 2010. Promoting social behavior with oxytocin in high-functioning autism spectrum disorders. Proc Natl Acad Sci USA 107(9):4389–4394.

5. Meyer-Lindenberg A, Domes G, Kirsch P, Heinrichs M. 2011. Oxytocin and vasopressin in the human brain: Social neuropeptides for translational medicine. Nat Rev Neurosci 12(9):524–538.
6. Chaibva FA, Walker RB. 2007. Development and validation of a stability-indicating analytical method for the quantitation of oxytocin in pharmaceutical dosage forms. J Pharm Biomed Anal 43(1):179–185.
7. Karbiwnyk CM, Faul KC, Turnipseed SB, Andersen WC, Miller KE. 2008. Determination of oxytocin in a dilute IV solution by LC-MS(n). J Pharm Biomed Anal 48(3):672–677.
8. Mueller JM, Pierce JG, Davoll H, Duvigneaud V. 1951. The oxidation of oxytocin with performic acid. J Biol Chem 191(1):309–313.
9. Turner RA, Pierce JG, Duvigneaud V. 1951. The desulfurization of oxytocin. J Biol Chem 193(1):359–361.
10. Groot ANJA, Vree TB, Hogerzeil HV, Walker GJA. 1997. Stability of oral oxytocics in tropical climates: Results of simulation studies on oral ergometrine, oral methylergometrine, buccal oxytocin and buccal desamino-oxytocin. Geneva, Switzerland: World Health Organization.
11. Hawe A, Poole R, Romeijn S, Kasper P, Heijden R, Jiskoot W. 2009. Towards heat-stable oxytocin formulations: Analysis of degradation kinetics and identification of degradation products. Pharm Res 26(7):1679–1688.
12. Avanti C, Amorij J-P, Setyaningsih D, Hawe A, Jiskoot W, Visser J, Kedrov A, Driessen AJM, Hinrichs WLJ, Frijlink HW. 2011. A new strategy to stabilize oxytocin in aqueous solutions: I. The effects of divalent metal ions and citrate buffer. AAPS J 13(2):284–290.
13. Poole RA, Kasper PT, Jiskoot W. 2011. Formation of amide- and imide-linked degradation products between the peptide drug oxytocin and citrate in citrate-buffered formulations. J Pharm Sci 100(7):3018–3022.
14. Hogerzeil HV, Walker GJA, de Goeje MJ. 1993. Stability of injectable oxytocics in tropical climates. Action Programme on Essential Drugs. Geneva, Switzerland: World Health Organization, pp 1–50.
15. Cesarini JP, Court L, McKinlay A, Sliney D, Selgrade MJ, Johnson G, Armstrong B, Van Loveren H, Koppikar A, Tyrrell RM, van der Leun JC, Badr IA, Kulandaivelu G. 1994. Environmental Health Criteria (EHC) 160: Ultraviolet radiation. Geneva, Switzerland: World Health Organization.
16. Barrón LB, Waterman KC, Filipiak P, Hug GL, Nauser T, Schöneich C. 2004. Mechanism and kinetics of photoisomerization of a cyclic disulfide, trans-4,5-dihydroxy-1,2-dithiacyclohexane. J Phys Chem A 108(12):2247–2255.
17. Mozziconacci O, Kerwin B, Schöneich C. 2010. Photolysis of an intrachain peptide disulfide bond: Primary and secondary processes, formation of H_2S, and hydrogen transfer reactions. J Phys Chem B 114(10):3668–3688.
18. Mozziconacci O, Haywood J, Gorman EM, Munson E, Schöneich C. 2012. Photolysis of recombinant human insulin in the solid state: Formation of a dithiohemiacetal product at the C-terminal disulfide bond. Pharm Res 29(1):121–133.
19. Mozziconacci O, Kerwin BA, Schöneich C. 2010. The exposure of a monoclonal antibody, IgG1, to UV-light leads to protein dithiohemiacetal and thioether cross-links. Chem Res Toxicol 23(8):1310–1312.
20. Lepre AM, Sutherland JC, Trunk JG, Sutherland BM. 1998. A robust, inexpensive filter for blocking UVC radiation in broad-spectrum 'UVB' lamps. J Photochem Photobiol B 43(1):34–40.
21. Ikehata K, Duzhak TG, Galeva NA, Ji T, Koen YM, Hanzlik RP. 2008. Protein targets of reactive metabolites of thiobenzamide in rat liver *in vivo*. Chem Res Toxicol 21(7):1432–1442.
22. Pharmeuropa. 1990. The European Pharmacopoeia Forum. Strasbourg: Council of Europe, pp 38–45.
23. Wysocki VH, Tsaprailis G, Smith LL, Breci LA. 2000. Mobile and localized protons: A framework for understanding peptide dissociation. J Mass Spectrom 35(12):1399–1406.
24. Thompson SD, Carroll DG, Watson F, O' Donnell M, McGlynn SP. 1966. Electronic spectra and structure of sulfur compounds. J Chem Phys 45(5):1367–1379.
25. Autrey T, Devadoss C, Sauerwein B, Franz JA, Schuster GB. 1995. Solvent cage recombination of 4-benzoylphenylthiyl radicals: Fast intersystem crossing of triplet sulfur-centered radical pairs. J Phys Chem 99(3):869–871.
26. Mozziconacci O, Sharov V, Williams TD, Kerwin BA, Schöneich C. 2008. Peptide cysteine thiyl radicals abstract hydrogen atoms from surrounding amino acids: The photolysis of a cystine containing model peptide. J Phys Chem B 112(30):9250–9257.
27. Fung YM, Kjeldsen F, Silivra OA, Chan TW, Zubarev RA. 2005. Facile disulfide bond cleavage in gaseous peptide and protein cations by ultraviolet photodissociation at 157 nm. Angew Chem Int Ed Engl 44(39):6399–6403.
28. Hug GL, Janeba-Bartoszewicz E, Filipiak P, Pedzinski T, Kozubek H, Marciniak B. 2008. Evidence for heterolytic cleavage of C-S bonds in the photolysis of 1,3,5-trithianes. Polish J Chem 82:883–892.
29. Janeba-Bartoszewicz E, Hug GL, Andrzejewska E, Marciniak B. 2006. Photochemistry of 1,3,5-trithianes in solution: Steady-state and laser flash photolysis studies. J Photochem Photobiol A 177(1):17–23.
30. Burdzinski G, Marciniak B. 2008. Photoinduced ultrafast ring-opening reaction in trithianes in solution. Chem Phys Lett 465(1–3):45–47.
31. Asmus KD, Hug GL, Bobrowski K, Mulazzani QG, Marciniak B. 2006. Transients in the oxidative and H-atom-induced degradation of 1,3,5-trithiane. Time-resolved studies in aqueous solution. J Phys Chem A 110(29):9292–9300.